REVIEW ARTICLE
OPEN ACCESS

REVISTA RIICS Investigación e innovación en ciencias de la salud

Comparative Optical Performance of Brain Tissue-Clearing Methods Combined with Immunostaining: A Systematic Review with Descriptive Quantitative Synthesis

Comparación del rendimiento óptico de los métodos de aclaramiento tisular cerebral combinados con inmunotinción: revisión sistemática con síntesis cuantitativa descriptiva

Jorge L. Anaya-González[1], **Claudia Velásquez-Calderón**[1], **AdrianaEdit MinietCastillo**[1], **Juan José Chingal-Cando**[1]

[1]*Facultad de Ciencias de la Salud, Universidad Técnica del Norte, Ibarra, Ecuador.*

Correspondence
Jorge L. Anaya-González.
Email: jlanaya@utn.edu.ec

Editor
Fraidy-Alonso Alzate-Pamplona, MSc.

Declaration of interests
The authors declare no conflicts of interest.

Funding
This research received no external funding.

Ethics statement
Ethical approval was not required for this study because it did not involve human participants, animals, or identifiable personal data.

Abstract

Introduction. Optical clearing has enabled three-dimensional visualization of brain tissue, but available methods differ in their ability to preserve morphology, achieve maximum effective imaging depth, and maintain fluorescent signal quality while minimizing unwanted background fluorescence.

Objective. To evaluate the optical and morphological performance of tissue-clearing protocols applied to immunostained brain structures through a systematic review with descriptive quantitative synthesis of studies published between 2014 and 2024.

Method. Experimental studies using human or rodent brain tissue combining optical clearing and immunostaining were identified through searches in Scopus and Web of Science following the PRISMA 2020 guidelines. Data were synthesized using descriptive statistics, group comparisons, non-parametric correlations, and exploratory regression analyses. Bibliometric network analyses were conducted using the software VOSviewer.

Results. Twelve experimental studies met the inclusion criteria. Organic solvent–based methods (iDISCO+, uDISCO) showed higher descriptive values of maximum effective imaging depth and lower levels of unwanted background fluorescence compared to hydrogel-based and hydrophilic approaches. Maximum effective imaging depth was significantly associated with reduced unwanted background fluorescence ($\rho = -0.596$; $p = 0.041$), while its association with fluorescent signal quality showed a non-significant positive trend ($\rho = 0.570$; $p = 0.053$).

Data availability
All data supporting the findings of this study are available within the article. For additional details, please contact the corresponding author.

Author Contributions
Jorge L. Anaya-González: conceptualization, data curation, formal analysis, investigation, methodology, project administration, resources, software, supervision, validation, visualization, writing – original draft, writing – review & editing.
Claudia Velásquez-Calderón: data curation, formal analysis, investigation, validation.
AdrianaEdit MinietCastillo: data curation, formal analysis, investigation, methodology, validation, writing – review & editing.
Juan José Chingal-Cando: data curation, formal analysis, investigation, software, validation.

Generative AI declaration
During the preparation of this manuscript, the authors used ChatGPT as a generative artificial intelligence tool solely for language editing. The tool was not used to generate scientific content, interpret results, create figures, or perform data analyses. The authors reviewed and edited the manuscript and take full responsibility for the accuracy and integrity of the final content.

Cite this article
Anaya-González JL, Velásquez-Calderón C, MinietCastillo A, Chingal-Cando JJ. Comparative optical performance of brain tissue-clearing methods combined with immunostaining: a systematic review with descriptive quantitative synthesis. Revista de Investigación e Innovación en Ciencias de la Salud. 2026;8(2):1-27. e-v8n2a532. https://doi.org/10.46634/riics.532

Received: 10/27/2025
Revised: 12/01/2025
Accepted: 03/05/2026
Published: 03/20/2026

Disclaimer
The content of this article is the sole responsibility of the authors and does not necessarily represent the official views of their affiliated institutions or the *Revista de Investigación e Innovación en Ciencias de la Salud*.

Conclusion. Organic solvent–based clearing methods exhibited more favorable descriptive optical profiles, particularly with respect to imaging depth and background suppression. However, in the absence of statistically significant between-group differences, these findings should be interpreted as suggestive patterns rather than definitive evidence of superiority.

Keywords

Optical clearing; immunostaining; brain tissue; fluorescence; three-dimensional microscopy; tissue transparency.

Resumen

Introducción. El aclaramiento óptico ha permitido la visualización tridimensional del tejido cerebral; sin embargo, los métodos disponibles difieren en su capacidad para preservar la morfología, alcanzar mayores profundidades de visualización efectiva y mantener una adecuada calidad de señal fluorescente con mínima fluorescencia de fondo no deseada.

Objetivo. Evaluar el rendimiento óptico y morfológico de los protocolos de aclaramiento tisular aplicados a tejido cerebral inmunotintado mediante una revisión sistemática con síntesis cuantitativa descriptiva de estudios publicados entre 2014 y 2024.

Método. Se identificaron estudios experimentales en tejido cerebral humano o murino que combinaron aclaramiento tisular e inmunotinción, mediante búsquedas en las bases de datos de Scopus y Web of Science, siguiendo las directrices PRISMA 2020. Se realizaron análisis descriptivos, comparaciones de grupos, correlaciones no paramétricas y modelos de regresión exploratorios. Se incluyó además un análisis bibliométrico con VOSviewer.

Resultados. Doce estudios cumplieron los criterios de inclusión. Los métodos basados en solventes orgánicos (iDISCO+, uDISCO) mostraron mayores valores descriptivos de profundidad máxima de visualización efectiva y menores niveles de fluorescencia de fondo no deseada en comparación con los métodos hidrofílicos y basados en hidrogel. La profundidad máxima de visualización efectiva se asoció significativamente con la reducción de fluorescencia de fondo no deseada ($\rho = -0{,}596$; $p = 0{,}041$), mientras que su relación con la calidad de la señal fluorescente mostró una tendencia positiva no significativa ($\rho = 0{,}570$; $p = 0{,}053$).

Conclusión. Los métodos de aclaramiento basados en solventes orgánicos presentaron perfiles ópticos descriptivamente más favorables, especialmente en profundidad de visualización y supresión de fondo. No obstante, estos hallazgos deben interpretarse como patrones sugerentes y no como evidencia concluyente de superioridad.

Palabras clave

Aclaramiento óptico; inmunotinción; tejido cerebral; fluorescencia; microscopía tridimensional; transparencia tisular.

Introduction

Achieving a three-dimensional visualization of brain microarchitecture remains a major technical challenge, with direct implications for clinical and translational neuroscience. Volumetric imaging of immunostained brain tissue enables improved detection of pathological changes associated with neurodegenerative disorders, enhances the characterization of neuronal and glial alterations in neuropathology, and supports circuit-level mapping in experimental disease models. These advances contribute to improved diagnostic interpretation, a better understanding of disease progression, and the development of targeted neurorehabilitation and neurological interventions [1–3]. Consequently, methodological advances in tissue clearing and volumetric immunostaining are highly relevant to health sciences and clinical research.

Conventional histological approaches rely on serial sectioning, which disrupts spatial continuity and introduces distortions in neuronal pathways. In contrast, optical tissue-clearing techniques reduce light scattering through lipid removal and refractive index homogenization, allowing deeper imaging of intact samples and improved visualization of neuronal and glial networks [4–7].

Over the past decade, tissue-clearing technologies have expanded considerably, giving rise to four broadly recognized methodological categories. Hydrogel-based protocols (e.g., CLARITY), are generally reported to preserve protein structure and tissue architecture while enabling moderate maximum effective imaging depth. Hydrophilic or aqueous methods such as CUBIC and SeedDB are often described as offering a balance between optical transparency and volumetric stability. Organic solvent-based approaches (e.g., iDISCO+, uDISCO, PEGASOS) are frequently associated with greater optical penetration, although potential trade-offs such as tissue shrinkage or reduced fluorescence retention have been reported. Hybrid or expansion-based techniques, including ProExM, combine chemical clearing with physical expansion to enable subcellular-resolution imaging. Each category presents distinct advantages and limitations related to optical transparency, structural preservation, and compatibility with immunostaining [5,8–13].

Newer rapid-clearing strategies have also been proposed in recent years; however, these were not represented among the studies meeting the eligibility criteria of the present review and are mentioned here solely for contextual completeness.

Despite these methodological advances, substantial variability persists across studies, particularly in antibody penetration efficiency, fluorescent signal quality, unwanted background fluorescence, and microscopy configurations [7,14–18]. In postmortem human brain tissue, adaptations of clearing and immunostaining protocols have enabled multicolour labelling and visualization of deep cortical structures. Nevertheless, challenges related to autofluorescence, incomplete labelling, and structural distortion remain significant [19–21].

The marked heterogeneity across studies (including differences in antibody selection, clearing chemistry, imaging modalities, and definitions of optical outcomes), limits the applicability of conventional effect-size-based meta-analytic approaches. To address this complexity, the present work applies a descriptive quantitative synthesis, integrating pooled summary statistics, correlation analyses, and exploratory regression models to characterize patterns of optical performance across clearing categories. This approach enables structured comparison while respecting the diversity of experimental designs and measurement frameworks reported in the literature.

Although several studies have reported partial quantitative comparisons of optical clearing performance, these analyses are often limited in scope and are not integrated into a unified synthesis focused specifically on immunostained brain tissue. Key outcome measures, such as maximum effective imaging depth, fluorescent signal quality, unwanted background fluorescence, and morphological preservation are inconsistently reported, hindering the development of evidence-informed guidance for protocol selection [22–25].

To address this gap, the present study conducts a systematic review with descriptive quantitative synthesis of tissue-clearing protocols combined with immunostaining in human and rodent brain samples. Maximum effective imaging depth, fluorescent signal quality, unwanted background fluorescence, and morphological preservation are comparatively examined across hydrogel-based, hydrophilic, solvent-based, and hybrid methods. By integrating data from heterogeneous experimental studies, this work aims to identify descriptive patterns of optical performance associated with different clearing strategies, and to support more informed methodological decision-making in three-dimensional neuroimaging research.

Objectives, Research Questions and Hypotheses

General Objective

To evaluate the optical and morphological performance of tissue-clearing protocols applied to immunostained brain structures (specifically, maximum effective imaging depth, fluorescent signal quality, unwanted background fluorescence, and morphological preservation) through a systematic review with descriptive quantitative synthesis of studies published between 2014 and 2024.

Specific Objectives

1. To compare maximum effective imaging depth across clearing methods according to chemical class: hydrogel-based, hydrophilic, solvent-based, and hybrid.
2. To evaluate fluorescent signal quality and unwanted background fluorescence in relation to immunostaining conditions, including primary and secondary antibody combinations.
3. To examine morphological preservation, including tissue shrinkage or expansion, and its association with clearing chemistry and optical performance.

Research Questions

Research questions were structured following the PICOC framework (Population, Intervention, Comparison, Outcome, Context), as outlined in Figure 1.

1. Which clearing chemistry is associated with greater maximum effective imaging depth in immunostained brain tissue?
2. How do different immunostaining conditions influence fluorescent signal quality and unwanted background fluorescence?
3. How does the chemical nature of each clearing method relate to morphological preservation in cleared brain tissue?
4. What associations are observed among maximum effective imaging depth, fluorescent signal quality, unwanted background fluorescence, and morphological preservation across clearing methods?

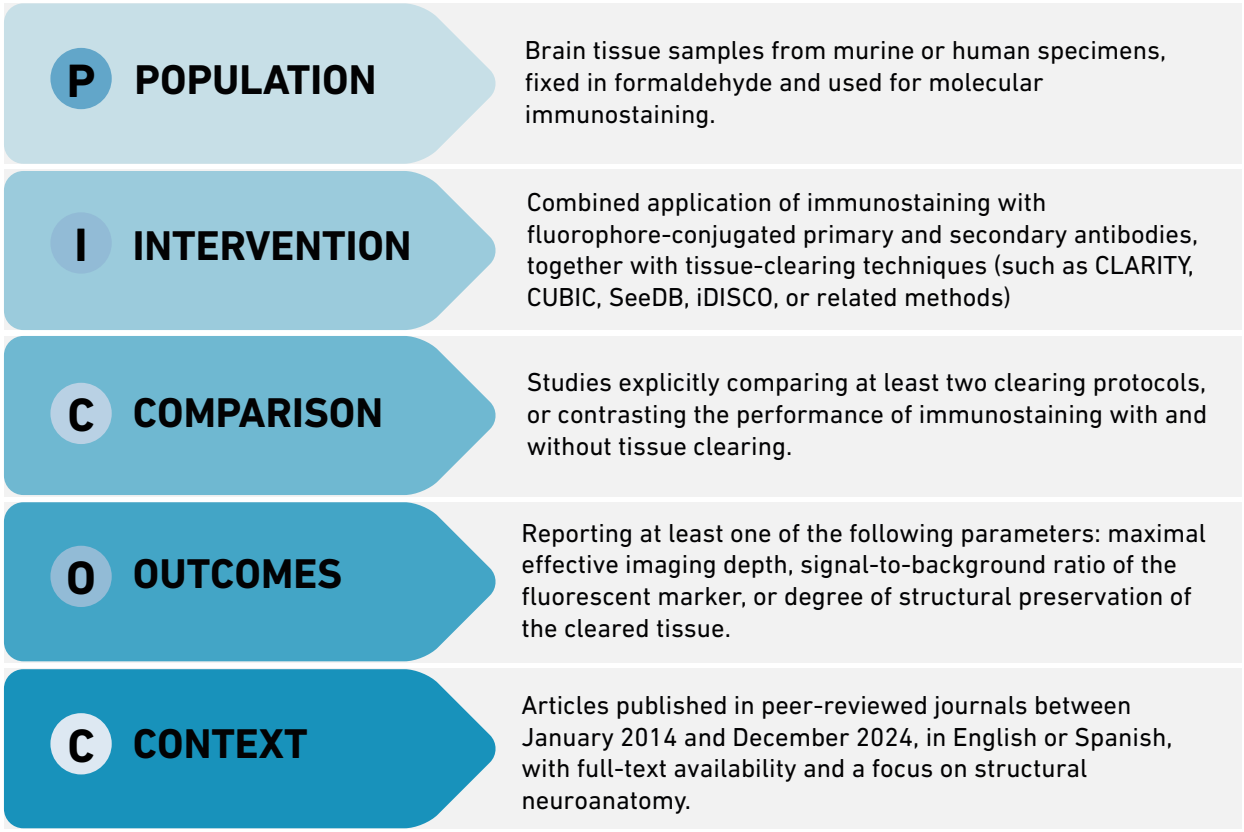

Figure 1. Elements for formulating the research question according to the PICOC framework.

Working Hypotheses

Based on the patterns reported in the literature, the following working hypotheses were formulated:

H1: Organic solvent-based tissue-clearing protocols are expected to be associated with greater maximum effective imaging depth compared with hydrogel-based, hydrophilic, and hybrid methods.

H2: Variations in fluorescent signal quality and unwanted background fluorescence are expected to depend on primary and secondary antibody combinations, with solvent-based methods hypothesized to show higher signal-to-background ratios under comparable conditions.

H3: Hydrogel-based and hydrophilic clearing protocols are expected to demonstrate better morphological preservation than organic solvent-based methods, despite achieving lower optical transparency.

H4: A positive association is hypothesized between maximum effective imaging depth and fluorescent signal quality, whereas an inverse association is anticipated between unwanted background fluorescence and overall optical performance.

Method

Study Design

A systematic review with descriptive quantitative synthesis was conducted in accordance with the PRISMA 2020 guidelines (Preferred Reporting Items for Systematic Reviews and Meta-Analyses) [26]. The methodological guidance provided by the *Cochrane Handbook for Systematic Reviews of Interventions* was followed to ensure transparency and reproducibility [27].

The protocol was prospectively registered in the International Prospective Register of Systematic Reviews (PROSPERO; CRD420251160314) [28]. The registration predefined the study objectives, research questions, eligibility criteria, and analytical approach. An administrative update was recorded on October 31, 2025, to clarify eligibility criteria and data synthesis procedures without modifying the original research objectives.

Study Classification

- Study type: Systematic review with descriptive quantitative synthesis
- Reporting framework: PRISMA 2020
- Methodological guidance: *Cochrane Handbook for Systematic Reviews of Interventions*
- Registration: PROSPERO (CRD420251160314)
- Time frame: January 2014 to December 2024

Information Sources

A comprehensive literature search was conducted in Scopus and Web of Science Core Collection covering publications from January 2014 to December 2024. Searches were limited to studies published in English or Spanish. Reference lists of all eligible articles were manually screened to identify additional relevant studies.

Although a complete search strategy was initially developed for PubMed/MEDLINE, a preliminary overlap assessment demonstrated that all PubMed-indexed records relevant to optical clearing and immunostaining were also retrieved through Scopus or Web of Science (WOS). Because these two databases yielded additional relevant studies not indexed in PubMed, the final search was restricted to WOS and Scopus to avoid redundancy while maintaining completeness.

Search Strategy

Search terms were constructed using a combination of controlled vocabulary and free-text keywords, linked with Boolean operators (AND / OR) and adapted to the syntax of each database. Quotation marks were used to delimit exact phrases. The strategy was structured according to the PICOC framework, ensuring coverage of population, intervention, comparison, outcomes, and context (Table 1).

PICOC-derived terms were applied to titles, abstracts, and keywords. The final search strategies are detailed below.

Table 1. Classification of search terms according to the PICOC framework.

PICOC Category	Search Descriptors	Purpose of the search
Population	*"human brain tissue", "murine brain tissue", "formaldehyde-fixed tissue"*	Defines the target population: human or murine brain tissue, fixed or postmortem.
Intervention	*"CLARITY", "CUBIC", "SeeDB", "tissue clearing"*	Identifies the main intervention: application of different tissue-clearing methods.
Comparator	*"comparative studies", "comparison between clearing protocols"*	Represents the comparison between distinct tissue-clearing protocols or methods.
Outcomes	*"structural preservation", "imaging depth", "signal-to-noise ratio"*	Corresponds to the primary outcomes defined in the PROSPERO protocol.
Context	*"3D brain visualization with immunolabeling", "molecular staining", "neuroimaging with molecular markers", "visualizing brain structures at molecular resolution"*	Delineates the experimental and technological context of the studies.
Complementary Technical Terms	*"fluorophore-conjugated antibodies", "immunofluorescence", "immunostaining"*	Refines the search by including fluorescent immunolabeling techniques associated with tissue-clearing protocols
Applied Filters	*LIMIT-TO (LANGUAGE, "English") OR LIMIT-TO (LANGUAGE, "Spanish") PUBYEAR > 2013 AND PUBYEAR < 2025*	Restricts the search to recent publications (2014–2024) in English or Spanish, corresponding to the period following the introduction of the CLARITY method.

Scopus (TITLE-ABS-KEY)

(("3D brain visualization with immunolabeling" OR "molecular staining" OR "neuroimaging with molecular markers" OR "visualizing brain structures at molecular resolution" OR "human brain tissue" OR "murine brain tissue" OR "formaldehyde-fixed tissue")

AND ("fluorophore-conjugated antibodies" OR "immunofluorescence" OR "immunostaining" OR "CLARITY" OR "CUBIC" OR "SeeDB" OR "tissue clearing")

AND ("comparative studies" OR "comparison between clearing protocols") AND ("structural preservation" OR "imaging depth" OR "signal-to-noise ratio")))

AND (LIMIT-TO (LANGUAGE, "English") OR LIMIT-TO (LANGUAGE, "Spanish")) AND (PUBYEAR > 2013 AND PUBYEAR < 2025))

Web of Science (TS)

(("3D brain visualization with immunolabeling" OR "molecular staining" OR "neuroimaging with molecular markers" OR "visualizing brain structures at molecular resolution" OR "human brain tissue" OR "murine brain tissue" OR "formaldehyde-fixed tissue")

AND ("fluorophore-conjugated antibodies" OR "immunofluorescence" OR "immunostaining" OR "CLARITY" OR "CUBIC" OR "SeeDB" OR "tissue clearing")

AND ("comparative studies" OR "comparison between clearing protocols")

AND ("structural preservation" OR "imaging depth" OR "signal-to-noise ratio"))

Prior to the final search, the strategy was piloted through scoping searches to ensure adequate sensitivity and confirm retrieval of key studies using alternative terminology. This iterative refinement minimized over-restriction while preserving conceptual specificity.

Eligibility Criteria

Inclusion

- Original experimental studies.
- Studies combining tissue-clearing protocols or protocols with immunostaining (primary antibody plus fluorophore-conjugated secondary antibody).
- Human or murine brain tissue (fixed or postmortem).
- Reporting at least one predefined outcome: maximum effective imaging depth, fluorescent signal quality, unwanted background fluorescence, or morphological preservation.
- Publications in peer-reviewed journals.

Exclusion

- Reviews, editorials, or methodological papers without original experimental data.
- Studies not employing optical clearing and immunostaining.
- Non-brain tissues or studies relying solely on endogenous fluorescence without antibody labeling.
- Incomplete reports or lack of full-text availability.
- Grey literature sources, conference abstracts, institutional repositories, and preprint servers.

Grey literature was intentionally excluded because optical performance metrics require validated, peer-review experimental protocols. The risk of publication bias was considered low due to redundancy across major citation databases and the consistent publication patterns observed in this field.

Selection Process and PRISMA Flow

Automatic database filters were applied prior to screening to restrict publication year (2014-2024), language (English or Spanish), and document type (original research articles). After duplicate removal, two independent reviewers screened titles and abstracts. All 27 records retained after automated filtering met the eligibility criteria and proceeded directly to full-text assessment.

At the full-text stage, eligibility criteria and methodological quality were evaluated concurrently. Methodological quality was assessed using the JBI Critical Appraisal Checklist. Studies rated as moderate or low quality, or failing eligibility criteria, were excluded. Fifteen

studies were excluded at this stage. The remaining 12 studies met all inclusion criteria and were rated as high quality, forming the final dataset for quantitative synthesis.

Discrepancies were resolved by consensus. Inter-rater agreement for quality assessment was excellent (Cohen´s $\kappa = 0.883$). The selection process is summarized in the PRISMA 2020 flow diagram [26] (Figure 2).

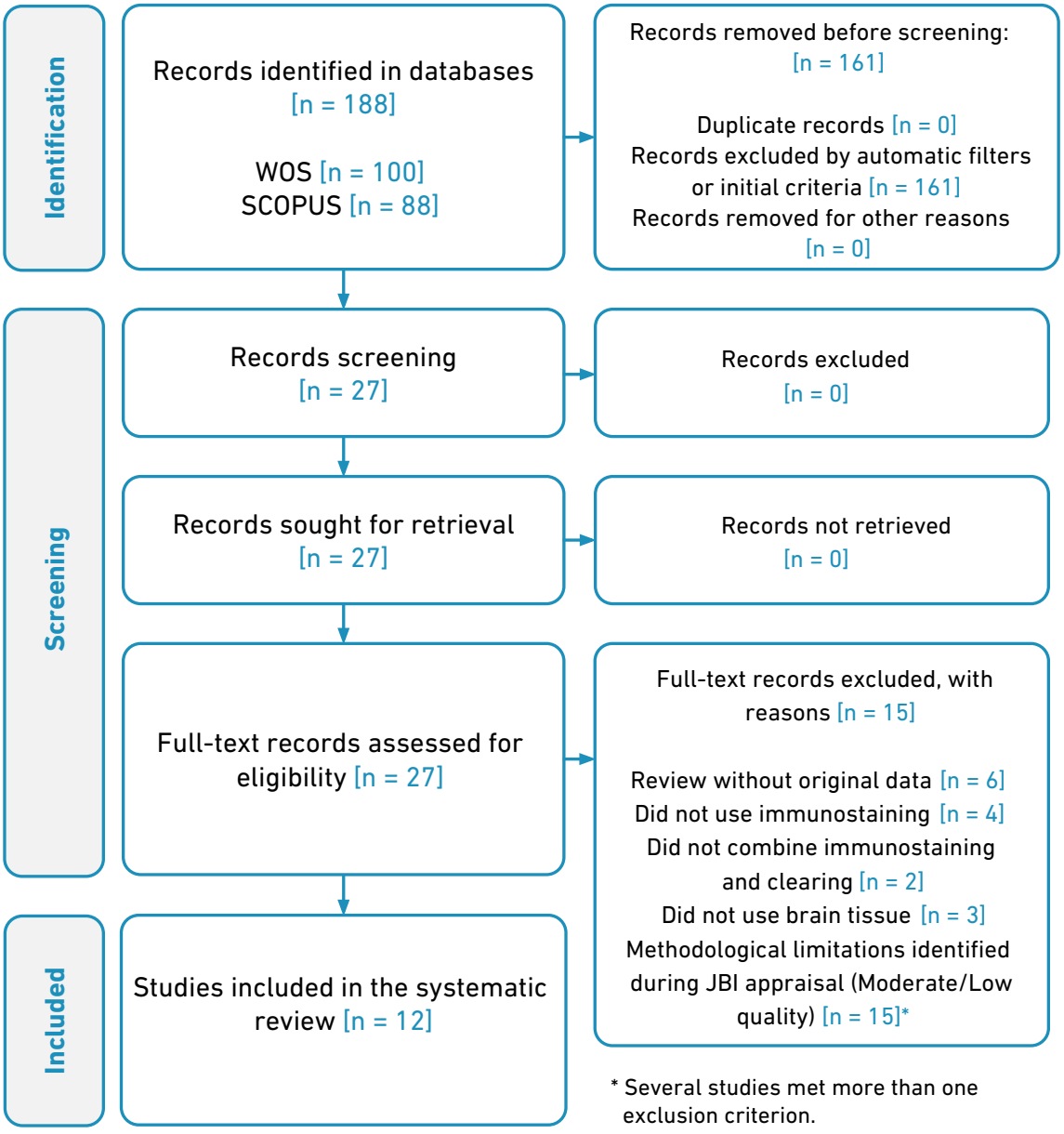

Figure 2. PRISMA Flow Diagram for the Study Selection Process.

Data Extraction and Coding

Data were extracted and coded into a structured database using SPSS v.29. Variables were categorized as follows:

- General variables: year, country, species, brain region, tissue type, processing time.
- Qualitative variables: clearing protocol, chemical principle, antibodies combinations, fluorophores, microscopy modality.
- Ordinal variables: morphological preservation, fluorescent signal quality, unwanted background fluorescence (three-level scale).
- Quantitative variable: maximum effective imaging depth (μm).

Methodological Quality Assessment

Methodological quality was independently assessed using the JBI Critical Appraisal Checklist for Quasi-Experimental Studies [29]. This tool was selected because the included studies consisted of heterogeneous laboratory experiments without randomization or clinical control groups.

Checklist items were operationalized to capture bias sources relevant to optical and imaging studies, including protocol reproducibility, control of technical variability, reliability of outcome measurements, and appropriateness of data analysis. Items were scored as fulfilled (1), partially fulfilled (0.5), or not fulfilled (0). Studies were classified as high (>80%), moderate (60-79%), or low (<60%) quality.

Only high-quality studies with complete optical outcome data were included. Inter-rater agreement was assessed using Cohen´s Kappa ($\kappa = 0.883$; $p<0.001$) (Table 2), indicating excellent agreement [30].

Table 2. Cohen´s Kappa and observed agreement for JBI quality assessment (n=27).

Quality		Reviewer 2			
		Low	Middle	High	Total
Reviewer 1	Low	**4 (80.0%)**	1 (20.0%)	0 (0.0%)	5 (100%)
	Middle	1 (10.0%)	**9 (90.0%)**	0 (0.0%)	10 (100%)
	High	0 (0.0%)	0 (0.0%)	**12 (100%)**	12 (100%)
	Total	5 (18.5%)	10 (37.0%)	12 (44.4%)	27 (100%)

Note. Cohen´s kappa = 0.883 (SE=0.078), p<0.001; observed agreement (Po): 92.6

Data Synthesis and Statistical Analysis

All analyses were conducted using SPSS version 29 and were predefined as descriptive and exploratory. Continuous variables were summarized using means and standard deviations, Normality and homoscedasticity were assessed using the Kolmogorov–Smirnov and Levene's tests, respectively.

Operationalization of outcome variables

Given the heterogeneity in outcome reporting, optical performance variables were harmonized using three-level ordinal scales (low, moderate, high). Quantitative measures and qualitative descriptions were mapped to these categories using predefined criteria based on relative performance within and across studies. When numerical values were unavailable, classification was achieved through independent reviewer consensus.

Ordinal variables were treated as quasi-continuous ones for exploratory comparisons, assuming approximately equidistant categories. This approach was adopted to identify global descriptive patterns rather than estimate precise effect sizes.

Group comparisons across chemical clearing categories were performed using one-way ANOVA or Welch's ANOVA, with post hoc testing (Tukey HSD or Games–Howell) as appropriate. Associations between optical outcomes were assessed using Spearman's rank correlation coefficient. Simple linear regression models were applied to explore potential functional relationships, with results interpreted as descriptive trends.

A p-value < 0.05 was considered statistically significant. Values between 0.05 and 0.10 were interpreted as non-significant trends. No correction for multiple comparisons was applied, given the exploratory nature of the analyses.

Heatmap visualizations were generated by averaging ordinal scores within antibody-protocol combinations. These averages were used exclusively for descriptive visualization and were not treated as continuous measures nor subjected to inferential testing. Direct statistical associations between fluorescent signal quality and unwanted background fluorescence were not independently tested.

Bibliometric Analysis

A descriptive bibliometric analysis was conducted using VOSviewer version 1.6.20 to examine keyword co-occurrence and co-authorship networks. Full counting was applied with a minimum occurrence threshold of one. Networks were interpreted based on frequency, link strength, and thematic clustering.

Ethical Considerations

This study involved no primary experimentation with human or animal subjects. All analyses were based exclusively on previously published data and adhered to international ethical guidelines for systematic reviews.

Results

Bibliometric and Network Analyses

The keywords co-occurrence analysis (Figure 3) identified two main thematic clusters. The red cluster grouped terms related to the physicochemical principles of optical clearing and immunostaining, reflecting the methodological focus of studies assessing optical performance. The green cluster comprised concepts associated with the neuroscientific application of clearing and immunostaining techniques. The connections between both clusters indicate that methodological and application-oriented concepts frequently co-occur within the included studies. Given the limited number of experimental articles included, this network should be interpreted primarily as an exploratory representation of thematic structure rather than as a comprehensive bibliometric mapping of the field.

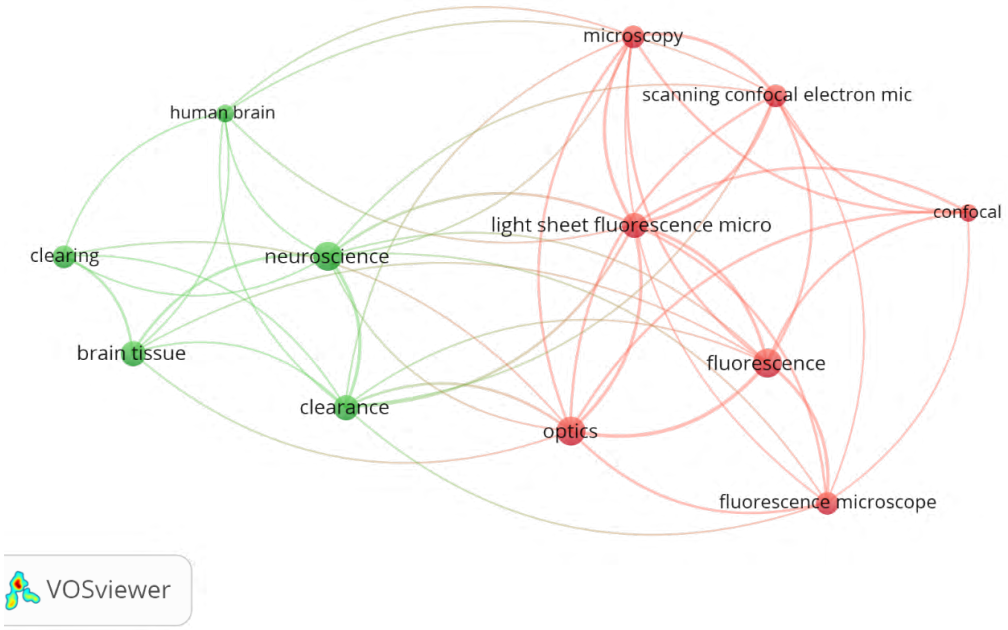

Figure 3. Co-occurrence network of keywords in research on optical clearing and three-dimensional brain imaging.

The co-authorship network (Figure 4) provides a descriptive overview of collaboration patterns among authors of the included studies. Each node represents an author, and links indicate shared publications. The network highlights recurrent collaborations among research groups working at the interface of neuroscience, biomedical optics, and tissue engineering. This analysis is presented for contextual purposes and does not imply differences in scientific contribution or methodological influence.

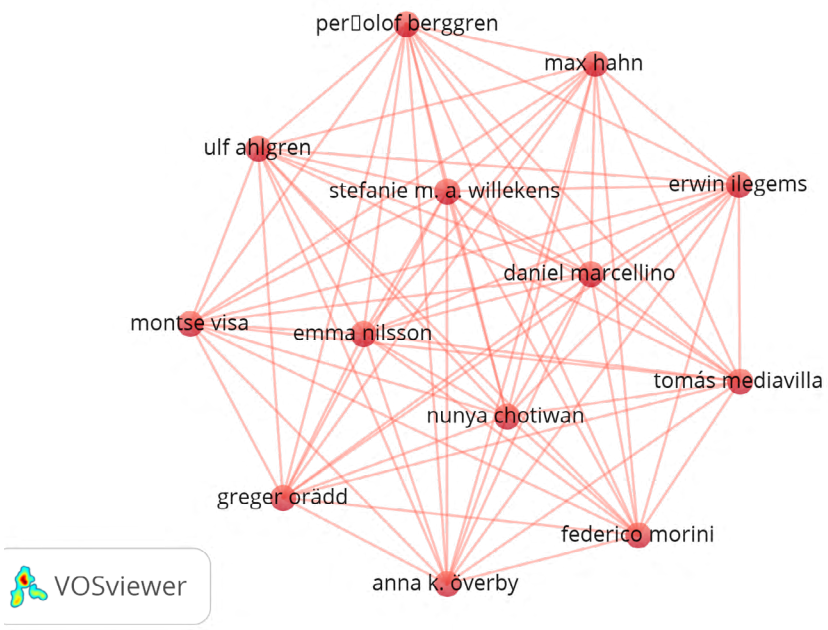

Figure 4. Co-authorship network of researchers involved in studies on brain tissue optical clearing.

Study characteristics

Table 3 summarizes the general characteristics of the 12 experimental studies published between 2014 and 2024 that were included in the quantitative synthesis. Nine studies (75%) were conducted in rodent brain tissue, while three (25%) examined human brain samples. A range of tissue-clearing protocols was represented, including CLARITY, CUBIC, SeeDB, iDISCO+, uDISCO, and ProExM. These methods corresponded to hydrogel-based, hydrophilic solution-based, organic solvent-based, and hybrid chemical principles.

Table 3. Summary of studies included in the systematic review.

Study	Brain structure/ Species	Tissue Type	Chemical principle*	Primary/ Secondary Antibody	Duration (days)	Microscopy
A novel, modernized Golgi-Cox stain optimized for CLARITY cleared tissue	Hippocampus/ Rodent	Fixed	Hydrogel	Anti-NeuN/ AF-488	11-14	Combined, Two-photon
An MR-based brain template and atlas for optical projection tomography and light sheet fluorescence microscopy in neuroscience	Whole brain/ Rodent	Fixed	Hydrogel	Anti-NeuN Anti-GFAP/ AF-594	11-14	Two-photon and LSFM
Brain pericytes acquire stemness via the nrf2-dependent antioxidant system	Striatum/ Rodent	Fixed	Organic Solvent	Anti-TH Anti-GFAP/ AF-594/647	7-10	LSFM
Clarifying clarity: quantitative optimization of the diffusion based delipidation protocol for genetically labeled tissue	Whole brain/ Rodent	Fixed	Hydrogel	Anti-NeuN/ AF-488	11-14	Combined
Comparative analyses of clearing efficacies of tissue clearing protocols by using a punching assisted clarity analysis	Hippocampus/ Rodent	Fixed	Hydrophilic	Anti-NeuN Anti-GFAP/ AF-594	7-10	Combined
Comparison of light-sheet fluorescence microscopy and fast-confocal microscopy for three- dimensional imaging of cleared mouse brain	Cortex/ Rodent	Fixed	Hydrophilic	Anti-GFAP/ AF-488	< 7	Laser Confocal
Fast 3-D imaging of brain organoids with a new single-objective planar-illumination two-photon microscope	Whole brain/ Rodent	Fixed	Organic Solvent	Anti-TH Anti-GAD67/ AF-594/647	7-10	LSFM
Immunofluorescent visualization of mouse interneuron subtypes.	Cortex/ Human	*Post mortem*	Hydrogel	Anti-NeuN Anti-GFAP/ AF-488	11-14	Combined

On-line optical clearing method for whole-brain imaging in mice	Whole brain/ Rodent	Fixed	Organic Solvent	Anti-NeuN/ AF-647	7-10	LSFM
Optimizing tissue clearing and imaging methods for human brain tissue	Cortex/ Human	*Post mortem*	Hydrogel	Anti-GFAP/ AF-488	11-14	Laser Confocal
Protein-retention expansion microscopy for visualizing subcellular organelles in fixed brain tissue	Hippocampus/ Rodent	Fixed	Hybrid	Anti-NeuN/ AF-488	<7	Combined
Scalable labeling for cytoarchitectonic characterization of large optically cleared human neocortex samples.	Cortex/ Human	*Post mortem*	Hydrophilic	Anti-NeuN Anti-MBP/ AF-647	>14	Combined

Notes. LSFM: Light Sheet Fluorescence Microscopy; AF: Alexa-Fluor; Combined: Laser Confocal + LSFM; * Chemical principle of optical clearing methods.

All clearing protocols were combined with immunostaining procedures using primary and fluorophore-conjugated secondary antibodies. Three-dimensional imaging was performed using various microscopy modalities, including two-photon microscopy, light-sheet fluorescence microscopy (LSFM), and confocal microscopy. The most frequently analyzed brain regions were the hippocampus, cerebral cortex, and whole brain preparations.

Volumetric changes and morphological preservation

Regarding volumetric tissue changes, a statistically non-uniform distribution across contraction and expansion categories was observed only among CLARITY-based protocols (Fisher´s exact test, $p = 0.048$). All CLARITY studies reported mild tissue contraction (-5% to -10%), with no severe contraction or expansion. Given the small number of studies and multiple categorical comparisons, this finding should be interpreted as an exploratory within-method pattern.

No statistically significant distributional differences were observed for volumetric changes in the remaining clearing methods. Percentages reported in Table 4 reflect relative distributions derived from small method-specific sample sizes. Fisher's exact test was applied because of low expected cell counts, and all results were interpreted descriptively.

Table 4. Comparison of morphological and optical variables according to the tissue-clearing method in immunostained brain tissue.

Variables		Optical clearing methods											
		CLARITY		CUBIC		SeeDB		uDISCO		iDISCO+		ProExM	
		%	*p**	%	*p**	%	*p**	%	*p**	%	*p**	%	*p**
Qualitative assessment of signal-to-background ratio	Moderate	60.0	0.558	33.3	—	50.0	—	0.0	—	0.0	0.470	0.0	—
	High	40.0		66.6		50.0		100.0		100.0		100.0	

Degree of structural preservation	Moderate	60.0	0.558	33.3	—	50.0	—	0.0	—	0.0	0.470	0.0	—
	High	40.0		66.6		50.0		100.0		100.0		100.0	
Visible morphological alterations	Mild	100.0	0.205	66.6	—	50.0	0.455	100.0	—	100.0	—	0.0	—
	Moderate	0.0		33.3		50.0		0.0		0.0		100.0	
Tissue volumetric change (%)	Severe Contraction (-25 to -30)	0.0	0.048	0.0	0.503	0.0	0.167	100.0	0.141	50.0	0.526	0.0	0.141
	Mild Contraction (-5 to -10)	100.0		66.6		50.0		0.0		50.0		0.0	
	Mild Expansion (5-10)	0.0		0.0		50.0		0.0		0.0		0.0	
	Moderate Expansion (15 - 25)	0.0		33.3		0.0		0.0		0.0		100.0	
Unwanted background fluorescence	Low	20.0	0.576	33.3	—	0.0	0.515	100.0	0.333	50.0	—	0.0	—
	High	80.0		66.6		100.0		0.0		50.0		100.0	
Fluorescent signal quality	Moderate	60.0	0.222	0.0	0.491	50.0	—	0.0	—	0.0	0.515	0.0	—
	High	40.0		100.0		50.0		100.0		100.0		100.0	
Maximum effective imaging depth (µm) [x̄±SD]		2860±1045		1540 ± 450		4333 ±1155		5000 ± —		4000 ± —		1200 ± —	

Notes. *Fisher test; — Invalid comparison.

Comparative statistical analyses

The Kolmogorov–Smirnov test with Lilliefors correction indicated a normal distribution for maximum effective imaging depth values (K–S = 0.147; p = 0.200), supporting the use of parametric methods for group comparisons.

Group-level comparisons of optical performance according to clearing methods, stratified by chemical principles, are presented in Table 5. Levene's test indicated heterogeneity of variances for fluorescent signal quality (p = 0.002), while the remaining variables met the assumption of homoscedasticity (p > 0.45). Neither one-way ANOVA nor Welch's ANOVA identified statistically significant differences between clearing categories for any of the analyzed outcomes (all p > 0.05). Consequently, observed differences across clearing categories are interpreted as descriptive patterns rather than statistically supported between-group effect.

Post hoc analysis using Games–Howell and Tukey HSD tests likewise showed no statistically significant pairwise differences (p ≥ 0.133). Effect size estimates (η^2) ranged from 0.16 to 0.27, corresponding to small-to-moderate magnitudes. These estimates provide only an approximate indication of effect size and should be interpreted as exploratory. Organic solvent-based methods showed the highest descriptive values for fluorescent signal quality and maximum effective imaging depth; however, these trends did not reach statistical significance.

Table 5. Comparative analysis of fluorescent signal quality, unwanted background fluorescence level, and maximum effective imaging depth according to the chemical principle of tissue-clearing methods.

Chemical principle of tissue-clearing methods	Fluorescent signal quality			Unwanted background fluorescence level			Maximum effective imaging depth (µm)		
	F o $\bar{\Delta}$	*p*	*95% CI*	*F o $\bar{\Delta}$*	*p*	*95% CI*	*F o $\bar{\Delta}$*	*p*	*95% CI*
Levene´s test (based on means)	15.65	0.002	-	0.387	0.691	-	0.877	0.452	-
ANOVA (classical)	1.455	0.289	-	0.773	0.493	-	0.996	0.411	-
Welch´s ANOVA	$\bar{\Delta}$=0			0.618	0.584	-	1.925	0.255	-
Post hoc	Games-Howell			Tukey HSD			Tukey HSD		
Hydrogel vs. Hydrophilic	0.267	0.805	[-1.72 – 1.18]	0.133	0.938	[-1.35 – 1.62]	206.6	0.98	[-3282.9 – 2869.6]
Hydrogel vs. Organic Solvents	0.600		[-1.47 – 0.27]	0.467	0.521	[-1.02 – 1.95]	1473.3	0.4	[-4549.6 – 1602.93]
Hydrophilic vs. Organic Solvents	0.333		[-2.30 – 1.63]	0.333	0.773	[-1.35 – 2.01]	1204.0	0.567	[-4706.0 – 2172.7]
Effect size (η^2)	0.266			0.161			0.199		

Note. $\bar{\Delta}$ = 0 (the variance is zero in at least one of the groups compared). The hybrid method was not included in the analysis, as it was applied in only one study.

Imaging depth distribution

Figure 5 presents a boxplot of maximum effective imaging depth by clearing chemistry. Organic solvent-based protocols exhibited the highest median imaging depths (approximately 4000–5000 µm) with relatively compact interquartile ranges. Hydrophilic methods showed the widest dispersion of value (approximately 1500-5000 µm). Hydrogel-based methods displayed intermediate maximum effective imaging depths (approximately 2500–3000 µm), whereas hybrid approaches showed the lowest optical penetration (<1500 µm).

Although an apparent ordering of median maximum effective imaging depth was observed across clearing categories, this pattern remained descriptive and was not supported by statistically significant group differences.

Heatmap analysis of optical quality

Figure 6 presents a descriptive heatmap illustrating the distribution of ordinal optical quality scores across primary-secondary antibody combinations and clearing chemistry. The displayed values represent mean descriptive scores derived from ordinal classifications and are used exclusively to facilitate visual comparison across categories.

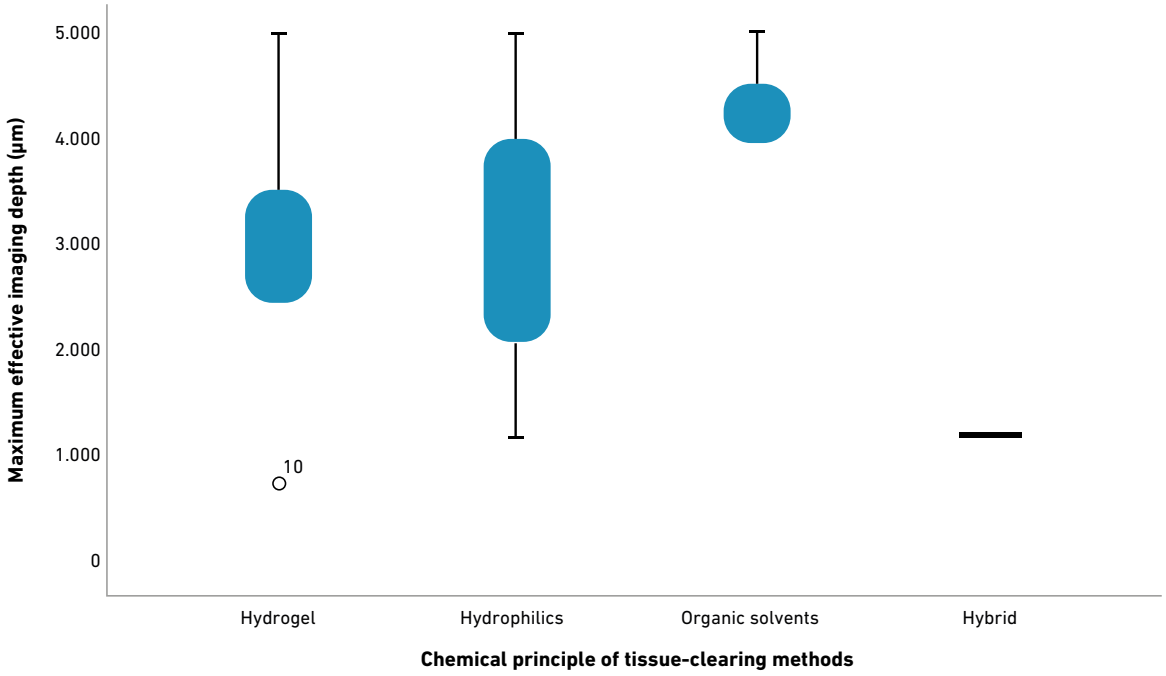

Figure 5. Distribution of maximum effective imaging depth (µm) according to the chemical principle of the tissue-clearing method.

Note: ANOVA: p>0.05; Tukey: p=0.426

Combination of primary and secondary antibodies	Chemical principle of the tissue-clearing method							
	Hydrogel	Hydrophilic solution	Organic solvents	Hybrid	Hydrogel	Hydrophilic solution	Organic solvents	Hybrid
	Fluorescent signal quality				Unwanted background fluorescence level			
NeuN–AF488	2.3			3	1.6			2
GFAP–AF488	2	2			1.5	2		
GFAP–AF594	3	3	3		2	2	2	
TH–AF594			3				1.5	
GAD67–AF647			3				1	
MBP–AF647		3				1		
NeuN–AF647		3	3			1	1	
Mean optical quality by chemical principle	2.4	2.8	3	3	1.7	1.5	1.4	2.0
Optical performance scale								
	Low			**High**	**low**			**High**

Figure 6. Optical performance according to the combination of primary and secondary antibodies and the chemical principle of tissue-clearing methods.

For fluorescent signal quality, higher intensity is represented in green and lower intensity in red. For unwanted background fluorescence, green denotes lower levels and red denotes higher levels.

Organic solvent–based protocols (iDISCO+, uDISCO) showed a higher proportion of antibody combinations classified as having high fluorescent signal quality and low unwanted background fluorescence, particularly for Alexa Fluor 594/647 conjugates (e.g., GFAP–AF594, TH–AF594, GAD67–AF647, NeuN–AF647). This distribution suggests a descriptive tendency toward higher fluorescent signal quality combined with lower unwanted background fluorescence under solvent-based clearing conditions.

Visual inspection of the heatmap indicates that higher signal quality scores frequently co-occur with lower unwanted background fluorescence levels. However, this apparent inverse association is based on descriptive visualization and was not evaluated using a direct statistical test between the two ordinal variables. Hydrophilic and hydrogel-based protocols more frequently exhibited moderate signal quality and unwanted background fluorescence categories, consistent with their emphasis on structural preservation. These heatmap findings align with, but do not independently confirm, the patterns observed in correlation and regression analyses involving maximum effective imaging depth.

Correlations and regression analyses

Spearman correlation revealed a moderate negative association between unwanted background fluorescence and maximum effective imaging depth, ($\rho = -0.596$; $p = 0.041$). In contrast, the association between maximum effective imaging depth and fluorescent signal quality did not meet the predefined threshold for statistical significance ($\rho = 0.570$; $p = 0.053$), although it showed a positive non-significant trend.

These results indicate that increased maximum effective imaging depth is significantly associated with reduced unwanted background fluorescence, whereas its relationship with fluorescent signal quality remains statistically inconclusive.

Simple linear regression analyses (Figure 7) showed that approximately 30% of the variability in fluorescent signal quality and 35% of the variability in unwanted background fluorescence were explained by maximum effective imaging depth ($R^2 = 0.3028$; $R^2 = 0.3533$, respectively). These models illustrate a direct relationship between maximum effective imaging depth and fluorescent signal quality and an inverse relationship with unwanted background fluorescence. Given the ordinal nature of the variables and the limited number of aggregated observations, these regression results should be considered exploratory and interpreted cautiously.

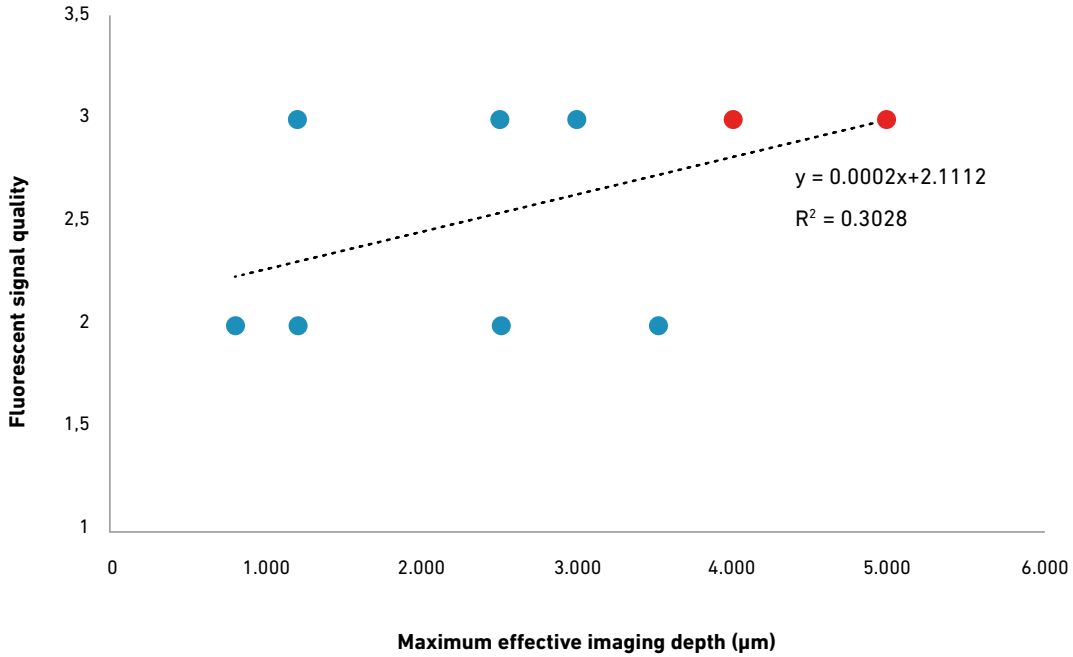

a) Relationship between maximum effective imaging depth (µm) and fluorescent signal quality ($\rho = 0.570$; $p = 0.053$).

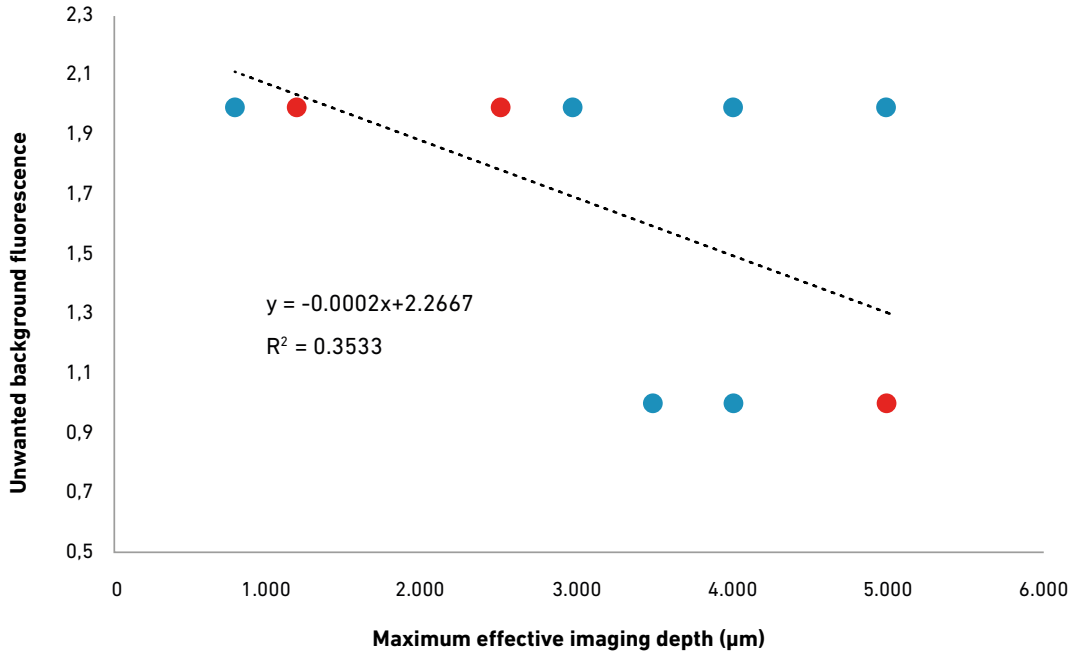

b) Relationship between maximum effective imaging depth (µm) and Unwanted background fluorescence ($\rho = -0.596$; $p = 0.041$).

Figure 7. Linear regression plots showing the bivariate correlations between maximum effective imaging depth, fluorescent signal quality, and unwanted background fluorescence.

Note: Overlapping data points are highlighted in red to improve visual clarity.

Discussion

This systematic review with descriptive quantitative synthesis provides a comparative evaluation of the principal optical clearing methods applied to immunostained brain tissue, integrating morphological and optical parameters. The results indicate that the chemical nature of the clearing method is associated with descriptive differences in maximum effective imaging depth, fluorescent signal quality, and unwanted background fluorescence. Across the analyzed studies, organic solvent–based protocols tended to exhibit higher optical performance in several descriptive outcomes, thereby supporting the study hypothesis at an exploratory level rather than demonstrating definitive superiority.

All comparative statements derived from this review should be interpreted as descriptive trends based on aggregated observations, rather than as evidence of statistically confirmed superiority or reference standards. The present findings are intended to inform methodological decision-making and hypothesis generation and do not establish definitive comparative effectiveness.

In the present descriptive synthesis, iDISCO+ and uDISCO tissue-clearing methods reached the highest reported maximum effective imaging depths (approximately 4000 µm) and exhibited high fluorescent signal quality. These findings are consistent with previous experimental reports, which have described the compatibility of these protocols with Alexa Fluor-conjugated antibodies in rodent brain tissue [28]. Although mechanistic parameters were not directly evaluated in this review, the higher optical performance observed for solvent-based methods is commonly attributed in the literature to efficient lipid removal and refractive index matching, which reduce internal light scattering and improve optical homogeneity [8,29-31]. These observations are presented as descriptive trends, given the absence of statistically significant differences in variance-based comparisons.

Hydrophilic solution–based methods, such as CUBIC and SeeDB, exhibited intermediate optical outcomes, while maintaining favourable morphological preservation. These patterns align with prior studies emphasizing their structural stability [2,32]. These protocols offer a balance between transparency and fluorophore compatibility, although they are associated with higher unwanted background fluorescence compared with organic solvent–based methods [11,33,34]. Hydrogel-based protocols, such as CLARITY, consistently preserved tissue architecture but achieved lower maximum effective imaging depth, likely due to constraints on light transmission and antibody diffusion imposed by the polymeric matrix [7,35-37]. Within the present datasets, the hybrid expansion-based ProExM technique was associated with high fluorescent signal quality but lower effective imaging depth. This trade-off has been more extensively characterized in previous studies, where physical expansion has been shown to enhance spatial resolution at the expense of total analysable volume [14,38,39].

Regarding associations between optical variables, a statistically significant negative correlation was observed between unwanted background fluorescence and maximum effective imaging depth ($\rho = -0.596$, $p = 0.041$). This finding indicates that increased tissue transparency is reliably associated with reduced unwanted background fluorescence. In contrast, the positive association between fluorescent signal quality and maximum effective imaging depth represented a non-significant trend ($\rho = 0.570$, $p = 0.053$) and should therefore be interpreted cautiously. These results are consistent with observations reported by Ueda et al., who attributed unwanted background fluorescence to the retention of endogenous pigments and aldehydes [1,40-43].

A study conducted in Wuhan reported a multiple linear regression model in which fluorescent signal quality and unwanted background fluorescence jointly accounted for more than 70% of the variance in maximum effective imaging depth. Although these findings were obtained under different experimental conditions, they provide a useful comparative framework for interpreting how clearing efficiency may influence photonic performance. In that context, organic solvents were described as acting as both delipidizing and refractive agents, contributing to enhanced optical homogeneity [19,44,45].

Heatmap analyses indicated that, within the analysed dataset, organic solvent-based methods were more frequently associated with antibody combinations classified as high fluorescent signal quality and low unwanted background fluorescence, particularly for Alexa Fluor 594/647 conjugates. These observations are descriptive in nature and align with, but do not independently confirm, the patterns identified in the statistical analyses. In this context, this tendency is consistent with the recommendations of Mai et al., who highlighted the advantage of high-photostability secondary antibodies in human postmortem brain studies [16,46-48].

Overall, all analysed clearing protocols exhibited satisfactory optical performance within their respective methodological context. Organic solvent–based methods tended to provide greater tissue transparency and higher fluorescent signal quality in descriptive comparisons. Hydrophilic solution–based methods offered a balance between structural preservation and optical penetration. Hydrogel-based protocols favoured morphological stability, whereas hybrid approaches emphasized maximal optical resolution. These patterns are consistent with prior methodological synthesis reported by Richardson and Lichtman [5,46].

Several limitations should be considered when interpreting these findings. Variability in primary and secondary antibody combinations, differences in microscopy techniques, and incomplete quantitative reporting contributed to experimental heterogeneity. In addition, fixation procedures were not consistently described across studies, which may have influenced optical outcomes [49-51]. Despite these constraints, the convergence of descriptive indicators across studies supports the internal coherence and descriptive robustness of the present quantitative synthesis.

In summary, this systematic review with descriptive quantitative synthesis indicates that optical clearing methods play a relevant role in shaping the visualization quality of immunostained brain tissue. Organic solvent–based methods consistently exhibited higher maximum effective imaging depth and favourable fluorescent signal quality in descriptive comparisons, albeit at the cost of moderate volumetric contraction. These methods may be considered a strong methodological option for three-dimensional neuroimaging studies in descriptive terms, particularly when optical transparency is prioritized over maximal morphological preservation. Future research should aim to improve immunological compatibility and minimize structural alterations to achieve an optimal balance between transparency, morphological preservation, and optical quality.

Limitations and Recommendations

Several limitations should be considered when interpreting the findings of this review.

First, substantial heterogeneity across studies was observed with respect to clearing chemistry, immunostaining conditions, imaging modalities, and definitions of optical outcomes. This variability limited direct comparability between studies and precluded the application of effect-size-based meta-analytic models.

Second, optical performance outcomes were harmonized using three-level ordinal classification schemes to accommodate heterogeneous reporting formats. Although this approach enabled structured synthesis, the subsequent use of descriptive and parametric statistical methods on ordinally coded data represents an additional methodological constraint that should be considered when interpreting comparative results.

Third, the quantitative associations identified between maximum effective imaging depth, fluorescent signal quality, and unwanted background fluorescence were exploratory in nature and derived from a small number of heterogeneous studies (n = 12). The exclusion of Moderate-and Low-quality studies based on JBI appraisal further reduced the effective sample size for correlation and regression analyses. Consequently, the reported correlation coefficients and R^2 values should be interpreted as indicative trends rather than stable predictive estimates.

Future research would benefit from standardized measurement criteria for tissue transparency, fluorescent signal quality, and unwanted background fluorescence, as well as from larger, well-controlled experimental datasets. In addition, systematic evaluation of hybrid protocols that aim to balance morphological preservation with optical performance may help address current methodological trade-offs and support more robust comparative analyses.

Conclusions

This systematic review with descriptive quantitative synthesis indicates that the chemical principle underlying tissue-clearing methods is associated with descriptive differences in optical performance and morphological preservation in immunostained brain tissue.

In descriptive comparisons, organic solvent-based methods tended to exhibit greater maximum effective imaging depth and favourable fluorescent signal characteristics, suggesting a potential advantage for three-dimensional neuroimaging applications. However, in the absence of statistically significant between-group differences and given the limited number of heterogeneous studies, these findings should be interpreted as indicative patterns rather than evidence of proven superiority.

Hydrophilic solution-based methods showed intermediate performance, balancing structural preservation and optical transparency, whereas hydrogel-based approaches consistently favoured morphological stability at the expense of maximum effective imaging depth. Hybrid expansion-based techniques achieved high subcellular resolution but were associated with reduced maximum effective imaging depth and were underrepresented in comparative analyses.

Increased maximum effective imaging depth was significantly associated with reduced unwanted background fluorescence, while its relationship with fluorescent signal quality did not reach statistical significance and should therefore be interpreted cautiously. Overall, the observed patterns suggest a possible functional interplay between tissue transparency and fluorescent signal quality characteristics, which requires confirmation in larger, standardized experimental datasets.

References

1. Ueda HR, Ertürk A, Chung K, Gradinaru V, Chedotal A, Tomancak P, et al. Tissue clearing and its applications in neuroscience. Nat Rev Neurosci [Internet]. 2020;21(2):61-79. doi: https://doi.org/10.1038/s41583-019-0250-1

2. Tainaka K, Kuno A, Kubota SI, Murakami T, Ueda HR. Chemical principles in tissue clearing and staining protocols for whole-body cell profiling. Annu Rev Cell Dev Biol [Internet]. 2016;32:713-41. doi: https://doi.org/10.1146/annurev-cellbio-111315-125001

3. Feng W, Liu C, Wang L, Zhang C. An optical clearing imaging window: Realization of mouse brain imaging and manipulation through scalp and skull. J Cereb Blood Flow Metab [Internet]. 2023;43(12):2105-119. doi: https://doi.org/10.1177/0271678X231167729

4. Hamer D, Petrinec D, Berecki M, Glasnović A, Gajović S. Tissue optical clearing methods for microscopy: A review of their application in neuroscience. Period Biol [Internet]. 2023;125(1-2):115-21. doi: https://doi.org/10.18054/pb.v125i1-2.24860

5. Richardson D, Lichtman JW. Clarifying tissue clearing. Cell [Internet]. 2015;162(2):246-57. doi: https://doi.org/10.1016/j.cell.2015.06.067

6. Yu T, Zhong X, Li D, Zhu J, Tuchin VV, Zhu D. Delivery and kinetics of immersion optical clearing agents in tissues: Optical imaging from ex vivo to in vivo. Adv Drug Deliv Rev [Internet]. 2024;215:115470. doi: https://doi.org/10.1016/j.addr.2024.115470

7. Du H, Hou P, Zhang W, Li Q. Advances in CLARITY-based tissue clearing and imaging (Review). Exp Ther Med [Internet]. 2018;16(3):1567-76. doi: https://doi.org/10.3892/etm.2018.6374

8. Zhao J, Lai HM, Qi Y, He D, Sun H. Current Status of Tissue Clearing and the Path Forward in Neuroscience. ACS Chem Neurosci [Internet]. 2021;12(1):5-29. doi: https://doi.org/10.1021/acschemneuro.0c00563

9. Muza PM, Perez M, Noy S, Kurosawa M, Katsouri L, Tybulewicz VLJ, et al. Affordable optical clearing and immunolabelling in mouse brain slices. BMC Res Notes [Internet]. 2023;16(1):246. doi: https://doi.org/10.1186/s13104-023-06511-y

10. Liang X, Luo H. Optical tissue clearing: Illuminating brain function and dysfunction. Theranostics [Internet]. 2021;11(7):3035-51. doi: https://doi.org/10.7150/thno.53979

11. Rocha MD, During DN, Bethge P, Voigt FF, Hildebrand S, Helmchen F, et al. Tissue clearing and light sheet microscopy: Imaging the unsectioned adult zebra finch brain at cellular resolution. Front Neuroanat [Internet]. 2019;13:13. doi: https://doi.org/10.3389/fnana.2019.00013

12. Kim K, Na M, Oh K, Cho E, Han SS, Chang S. Optimized single-step optical clearing solution for 3D volume imaging of biological structures. Commun Biol [Internet]. 2022;5:431. doi: https://doi.org/10.1038/s42003-022-03388-8

13. Parra-Damas A, Saura CA. Tissue Clearing and Expansion Methods for Imaging Brain Pathology in Neurodegeneration: From Circuits to Synapses and Beyond. Front Neurosci [Internet]. 2020;14:914. doi: https://doi.org/10.3389/fnins.2020.00914

14. Tillberg P. Protein-retention expansion microscopy: Improved sub-cellular imaging resolution through physical specimen expansion. In: Guichard P, Hamel V, editors. Methods in Cell Biology [Internet]. Amsterdam: Elsevier; 2021. p. 1-14. doi: https://doi.org/10.1016/bs.mcb.2020.04.015

15. Alkemade A, Bazin PL, Balesar R, Pine K, Kirilina E, Moller H, et al. A unified 3D map of microscopic architecture and MRI of the human brain. Sci Adv [Internet]. 2022;8(17):1-9. doi: https://doi.org/10.1126/sciadv.abj7892

16. Mai H, Lu D. Tissue clearing and its applications in human tissues: A review. View [Internet]. 2024;5(2):20230046. doi: https://doi.org/10.1002/VIW.20230046

17. Scardigli M, Pesce L, Brady N, Mazzamuto G, Gavryusev V, Silvestri L, et al. Comparison of different tissue clearing methods for three-dimensional reconstruction of human brain cellular anatomy using advanced imaging Techniques. Front Neuroanat [Internet]. 2021;15:772234. doi: https://doi.org/10.3389/fnana.2021.752234

18. Rosen GA, Kirsch D, Nicks R, Kelley H, Mathias R, Cormier KA, et al. SHARD: an improved method for staining and visualizing multiplex immunofluorescence in optically cleared postmortem human brain tissue. Front Neurosci [Internet]. 2024;18:1474617. doi: https://doi.org/10.3389/fnins.2024.1474617

19. Zhu J, Liu X, Liu Z, Deng Y, Xu J, Liu K, et al. SOLID: minimizing tissue distortion for brain-wide profiling of diverse architectures. Nat Commun [Internet]. 2024;15:8303. doi: https://doi.org/10.1038/s41467-024-52560-7

20. Wan P, Zhu J, Xu J, Li Y, Yu T, Zhu D. Evaluation of seven optical clearing methods in mouse brain. Neurophotonics [Internet]. 2018;5(3):035007. doi: https://doi.org/10.1117/1.NPh.5.3.035007

21. Hamzah N, Lim SM, Lim FT, Khabooshan MA, Kaslin J, Majeed AB, et al. Comparative analysis of tissue-clearing methods for whole brain imaging of adult zebrafish using BABB, iDISCO, and ECi. J Neurosci Methods [Internet]. 2025;422:110520. doi: https://doi.org/10.1016/j.jneumeth.2025.110520

22. Mutschler A, Malechka VV, Bagaev N, Baranov P, Soucy JR. Optimizing tissue clearing methods for improved imaging of whole-mount retinas and optic nerves. J Neurosci Methods [Internet]. 2025;424:110563. doi: https://doi.org/10.1016/j.jneumeth.2025.110563

23. Page M, McKenzie JE, Bossuyt PM, Boutron I, Hoffmann TC, Mulrow CD, et al. The PRISMA 2020 statement: an updated guideline for reporting systematic reviews. BMJ [Internet]. 2021;372:n71. doi: https://doi.org/10.1136/bmj.n71

24. Higgins J, Thomas J, Chandler J, Cumpston M, Li T, Page M, et al, editors. Cochrane Handbook for Systematic Reviews of Interventions. 6.5 [Internet]. London: Cochrane; 2024 [cited 2025 oct 09]. Available from: https://www.cochrane.org/authors/handbooks-and-manuals/handbook

25. Anaya Gonzalez JL, Velasquez C, Miniet Castillo AE, Chingal J. Comparative optical performance of brain tissue-clearing methods combined with immunostaining: A systematic review and descriptive meta-analysis. PROSPERO 2025 CRD420251160314 [Internet]. 2025 [cited 2025 Oct 22]. Available from: https://www.crd.york.ac.uk/PROSPERO/view/CRD420251160314

26. Aromataris E, Lockwood C, Porritt K, Pila B, Jordan Z, editors. JBI Manual for Evidence Synthesis. JBI [Internet]. Adelaide: JBI; 2024 [cited 2025 oct 09]. doi: https://doi.org/10.46658/JBIMES-20-01

27. Landis J, Koch G. An Application of Hierarchical Kappa-type Statistics in the Assessment of Majority Agreement among Multiple Observers. Biometrics [Internet]. 1977;33(2):363-74. doi: https://doi.org/10.2307/2529786

28. Molbay M, Kolabas ZI, Todorov MI, Ohn TL, Erturk A. A guidebook for DISCO tissue clearing. Mol Syst Biol [Internet]. 2021;17:MSB20209807. doi: https://doi.org/10.15252/msb.20209807

29. Kim JH, Jang MJ, Choi J, Lee E, Song KD, Cho J, et al. Optimizing tissue-clearing conditions based on analysis of the critical factors affecting tissue-clearing procedures. Sci Rep [Internet]. 2018;8:12815. doi: https://doi.org/10.1038/s41598-018-31153-7

30. Yu T, Zhu J, Li D, Zhu D. Physical and chemical mechanisms of tissue optical clearing. iScience [Internet]. 2021;24(3):102178. doi: https://doi.org/10.1016/j.isci.2021.102178

31. Wang S, Ren X, Wang J, Peng Q, Niu X, Song C, et al. Blocking autofluorescence in brain tissues affected by ischemic stroke, hemorrhagic stroke, or traumatic brain injury. Front Immunol [Internet]. 2023;14:1168292. doi: https://doi.org/10.3389/fimmu.2023.1168292

32. Woo J, Lee EY, Lee M, Ku S, Park JY, Cho YE. Comparative analyses of clearing efficacies of tissue clearing protocols by using a punching assisted clarity analysis. Front Bioeng Biotechnol [Internet]. 2022;9:784626. doi: https://doi.org/10.3389/fbioe.2021.784626

33. Azaripour A, Lagerweij T, Scharfbillig C, Jadczak AE, Willershausen B, Van Noorden CJF. A survey of clearing techniques for 3D imaging of tissues with special reference to connective tissue. Prog Histochem Cytochem [Internet]. 2016;51(2):9-23. doi: https://doi.org/10.1016/j.proghi.2016.04.001

34. Kolesová H, Čapek M, Radochová B, Janáček J, Sedmera D. Comparison of different tissue clearing methods and 3D imaging techniques for visualization of GFP-expressing mouse embryos and embryonic hearts. Histochem Cell Biol [Internet]. 2016;146(2):141-52. doi: https://doi.org/10.1007/s00418-016-1441-8

35. Du H, Hou P, Wang L, Wang Z, Li Q. Modified CLARITY achieving faster and better intact mouse brain clearing and immunostaining. Sci Rep [Internet]. 2019;9:10571. doi: https://doi.org/10.1038/s41598-019-46814-4

36. Guo Z, Zheng Y, Zhang Y. CLARITY techniques based tissue clearing: types and differences. Folia Morphol (Warsz) [Internet]. 2022;81(1):1-12. doi: https://doi.org/10.5603/FM.a2021.0012

37. Gantar I, Nguyen J, Karamanlis D, Ceto S, Osterop SF, Rajot D, et al. Protocol for reproducible EZ clearing and labeling, including optimized steps and quantified fluorescence retention on mouse tissue. STAR Protoc [Internet]. 2025;6(4):104105. doi: https://doi.org/10.1016/j.xpro.2025.104105

38. Campbell LA, Pannoni KE, Savory NA, Lal D, Farris S. Protein-retention expansion microscopy for visualizing subcellular organelles in fixed brain tissue. J Neurosci Methods [Internet]. 2021;361:109285. doi: https://doi.org/10.1016/j.jneumeth.2021.109285

39. Aristova D, Kylies D, Del Rosario M, Heil HS, Schwerk M, Kuehl M, et al. Nanoscale imaging of biological systems via expansion and super-resolution microscopy. Appl Phys Rev [Internet]. 2025;12(2):021311. doi: https://doi.org/10.1063/5.0240464

40. Wang Y, Gu Y, Wang J, Xuan A, Kong C, Fang WQ, et al. Real-time self-supervised denoising for high-speed fluorescence neural imaging. Nat Commun [Internet]. 2025;16:9396. doi: https://doi.org/10.1038/s41467-025-64681-8

41. Wirth D, Kolste K, Kanick S, Roberts DW, Leblond F, Paulsen KD. Fluorescence depth estimation from wide-field optical imaging data for guiding brain tumor resection: a multi-inclusion phantom study. Biomed Opt Express [Internet]. 2017;8(8):3656-70. doi: https://doi.org/10.1364/BOE.8.003656

42. Dong C, Zheng Y, Long-Iyer K, Wright EC, Li Y, Tian L. Fluorescence imaging of neural activity, neurochemical dynamics, and drug-specific receptor conformation with genetically encoded sensors. Annu Rev Neurosci [Internet]. 2022;45:273-94. doi: https://doi.org/10.1146/annurev-neuro-110520-031137

43. Kim TH, Schnitzer MJ. Fluorescence imaging of large-scale neural ensemble dynamics. Cell [Internet]. 2022;185(1):9-41. doi: https://doi.org/10.1016/j.cell.2021.12.007

44. Li D, Hu Z, Zhang H, Yang Q, Zhu L, Liu Y, et al. A Through-Intact-Skull (TIS) chronic window technique for cortical structure and function observation in mice. eLight [Internet]. 2021;2:15. doi: https://doi.org/10.1186/s43593-022-00022-2

45. Zhu D, Larin KV, Luo Q, Tuchin VV. Recent progress in tissue optical clearing. Laser Photon Rev [Internet]. 2013;7(5):732-57. doi: https://doi.org/10.1002/lpor.201200056

46. Lai HM, Tang Y, Lau ZYH, Campbell RAA, Yau JCN, Chan CCY, et al. Antibody stabilization for thermally accelerated deep immunostaining. Nat Methods [Internet]. 2022;19(9):1137-46. doi: https://doi.org/10.1038/s41592-022-01569-1

47. Yin T, Yesiltepe M, Metkar S, Ramon A, Greenig M, Sormanni P, et al. The NewroBus platform: engineered humanized anti-TfR1 nanobodies for efficient brain delivery. Cell Commun Signal [Internet]. 2026;24:69. doi: https://doi.org/10.1186/s12964-025-02605-1

48. Shan QH, Qin XY, Zhou N, Huang C, Wang Y, Chen P, et al. A method for ultrafast tissue clearing that preserves fluorescence for multimodal and longitudinal brain imaging. BMC Biol [Internet]. 2022;20:77. doi: https://doi.org/10.1186/s12915-022-01275-6

49. Lee K, Lai HM, Soerensen MH, Hui ESK, Ma VWS, Cho WCS, et al. Optimised tissue clearing minimises distortion and destruction during tissue delipidation. Neuropathol Appl Neurobiol [Internet]. 2021;47(3):441-53. doi: https://doi.org/10.1111/nan.12673

50. Weiss KR, Voigt FF, Shepherd DP, Huisken J. Tutorial: practical considerations for tissue clearing and imaging. Nat Protoc [Internet]. 2021;16(6):2732-48. doi: https://doi.org/10.1038/s41596-021-00502-8

51. Zwang TJ, Bennett RE, Lysandrou M, Woost B, Zhang A, Lieber CM, et al. Tissue libraries enable rapid determination of conditions that preserve antibody labeling in cleared mouse and human tissue. eLife [Internet]. 2023;12:e84112 doi: https://doi.org/10.7554/eLife.84112